

Dynamical Mass Measurements of Pre-Main-Sequence Stars: Fundamental Tests of the Physics of Young Stars

R. D. Mathieu

University of Wisconsin – Madison

I. Baraffe

École Normale Supérieure, Lyon

M. Simon

State University of New York – Stony Brook

K. G. Stassun

Vanderbilt University

R. White

University of Alabama in Huntsville

There are now 23 dynamical mass measurements for PMS stars of less than $2 M_{\odot}$, with most of the measured stars having masses greater than $0.5 M_{\odot}$. The masses of two PMS brown dwarfs have also been precisely measured. The most important application of these dynamical mass measurements has been to provide tests of theoretical masses derived from PMS stellar evolution models. On average most models in use today predict stellar masses to within 20%; however, the predictions for individual stars can be in error by 50% or more. Now that dynamical mass measurements are relatively abundant, and will become more so with the application of ground-based optical/infrared interferometers, the primary limitations to such tests have become systematic errors in the determination of the stellar properties necessary for the comparison with evolutionary models, such as effective temperature, luminosity, and radii. *Additional dynamical mass determinations between $0.5 M_{\odot}$ and $2 M_{\odot}$ will not likely improve the constraints on evolutionary models until these systematic uncertainties in measurements of stellar properties are reduced.* The nature and origin of these uncertainties, as well as the dominant physical issues in theoretical PMS stellar evolution models, are discussed. There are immediately realizable possibilities for improving the characterizations of those stars with dynamical mass measurements. Additional dynamical mass measurements for stars below $0.5 M_{\odot}$ are also very much needed.

1. INTRODUCTION

Prior to the measurement by *Popper* (1987) of the mass of the pre-main-sequence (PMS) secondary of the eclipsing binary EK Cep, every mass cited for a PMS star had been derived by comparing the star's location in the HR-diagram to the predictions of theoretical evolutionary models, which track how a star of given mass evolves in luminosity and temperature with age. These theoretical assignments of stellar masses were entirely unconstrained by direct mass measurements of PMS stars. Furthermore, different models can predict masses that differ by as much as a factor two or more.

The masses so assigned to PMS stars are at the very foundation of our understanding of star and planet

formation. These masses define the initial mass function that delimits the outcome of the star formation process. They set the energy scale available to explain processes ranging from accretion to outflow. They allow us to link young stars with older generations. And these masses permit us to identify stars that can serve as proxies for the Sun-Earth system at an early age.

Equally importantly, stellar masses represent a key observational interface for theoretical stellar evolution models. Such models provide our chronology of early stellar evolution and thereby touch upon the most basic of questions, including the timescale for circumstellar disk evolution and planet formation.

Thus the importance of the measurement of accurate PMS stellar masses in order to test theoretical masses can hardly be overstated. As the authors of this paper, we have the good fortune to be writing one of the

Table 1: Dynamical Masses and Stellar Properties of 23 Pre-Main-Sequence Stars

Name	Mass (M_{\odot})	Type	Ref	Radius (R_{\odot})	SpT	Log (T_{eff})	Log (L/L_{\odot})	Ref
RS Cha A	1.858 ± 0.016	EB	A91	2.137 ± 0.055	A8	3.883 ± 0.010	1.144 ± 0.044	M00
RS Cha B	1.821 ± 0.018	EB	A91	2.338 ± 0.055	A8	3.859 ± 0.010	1.126 ± 0.043	M00
MWC 480	1.65 ± 0.07	DK	Si00	...	A2-3	3.948 ± 0.015	1.243 ± 0.10	HW
TY CrA B	1.64 ± 0.01	EB	C98	2.080 ± 0.140	...	3.690 ± 0.035	0.380 ± 0.145	C98
045251+3016 A	1.45 ± 0.19	AS	St01	...	K5	3.643 ± 0.015	-0.167 ± 0.053	St01
BP Tau	$1.32 + 0.20 / - 0.12^*$	DK	D03	...	K7	3.608 ± 0.012	-0.78 ± 0.10	J99
0529.4+0041 A	1.25 ± 0.05	EB	C00	1.700 ± 0.200	K1-2	3.701 ± 0.009	0.243 ± 0.037	C00
EK Cep B	1.124 ± 0.012	EB	P87	1.320 ± 0.015	...	3.755 ± 0.015	0.190 ± 0.070	P87
UZ Tau Ea	$1.016 \pm 0.065^*$	DKS	P02	...	M1	3.557 ± 0.015	-0.201 ± 0.124	P02
V1174 Ori A	1.009 ± 0.015	EB	S04	1.339 ± 0.015	K4.5	3.650 ± 0.011	-0.193 ± 0.048	S04
LkCa 15	$0.97 \pm 0.03^*$	DK	Si00	...	K5	3.643 ± 0.015	-0.165 ± 0.10	HW
0529.4+0041 B	0.91 ± 0.05	EB	C00	1.200 ± 0.200	...	3.604 ± 0.022	-0.469 ± 0.192	C00
GM Aur	$0.84 \pm 0.05^*$	DK	S01	...	K7	3.602 ± 0.015	0.598 ± 0.10	HW
045251+3016 B	0.81 ± 0.09	AS	St01	...	M2	3.535 ± 0.015	-0.830 ± 0.086	St01
V1174 Ori B	0.731 ± 0.008	EB	S04	1.065 ± 0.011	...	3.558 ± 0.011	-0.761 ± 0.058	S04
DL Tau	$0.72 \pm 0.11^*$	DK	Si00	...	K7-M0	3.591 ± 0.015	0.005 ± 0.10	HW
HD 98800 Ba	0.699 ± 0.064	AS	B05	3.623 ± 0.016	0.330 ± 0.075	B05
HD 98800 Bb	0.582 ± 0.051	AS	B05	3.602 ± 0.016	0.167 ± 0.038	B05
DM Tau	$0.55 \pm 0.03^*$	DK	Si00	...	M1	3.557 ± 0.015	-0.532 ± 0.10	HW
CY Tau	$0.55 \pm 0.33^*$	DK	Si00	...	M2	3.535 ± 0.015	-0.491 ± 0.10	HW
UZ Tau Eb	$0.294 \pm 0.027^*$	DKS	P02	...	M4	3.491 ± 0.015	-0.553 ± 0.124	HW
2M0535-05 A	0.0541 ± 0.0046	EB	S06	0.669 ± 0.034	M6.5	3.423 ± 0.016	-1.699 ± 0.078	S06
2M0535-05 B	0.0340 ± 0.0027	EB	S06	0.511 ± 0.026	...	3.446 ± 0.016	-1.848 ± 0.076	S06

References: A91=*Andersen 1991*; Si00=*Simon et al. 2000*; C98=*Casey et al. 1998*; St01=*Steffen et al. 2001*; D03=*Dutrey et al. 2003*; C00=*Covino et al. 2000*; P87=*Popper 1987*; P02=*Prato et al. 2002*; S04=*Stassun et al. 2004*; B05=*Boden et al. 2005*; S06=*Stassun et al. 2006*; M00=*Mamajek et al. 2000*; J99=*Johns-Krull et al. 1999*; HW=*Hillenbrand and White 2004*

Techniques: EB = Eclipsing Binary, DK = Disk Kinematics, AS = Astrometric and Spectroscopic, DKS = Disk Kinematics and Spectroscopic (to divide total mass in double-lined system)

* Asterisks indicate that an uncertainty in the distance is not included in the mass uncertainty.

first reviews of PMS masses in which much of the text discusses actual mass measurements for PMS stars, rather than what needs to be known and how that knowledge will be gained in the very near future!

This paper first reviews in Section 2 the present capabilities for dynamical mass measurements of PMS stars, with an emphasis on random and systematic uncertainties, and then summarizes the present dynamical mass measurements in Table 1. In Section 3 we compare these mass measurements with theoretical mass values, and note that theory tends to underpredict masses at a marginally significant level. A

key point of this paper is that the limitation in these comparisons has become the determination of accurate stellar properties (effective temperature, luminosity, and radius) by which to derive theoretical mass values for those stars with measured masses. The uncertainties in these stellar properties are also discussed in Section 3. Section 4 presents a review of present stellar evolution theory for very low mass stars and brown dwarfs, and identifies the primary physical issues for the theory. Finally, in Section 5 we briefly discuss the very bright future in this field.

2. DYNAMICAL MASS MEASUREMENTS

Dynamical analyses applied to Keplerian motions of companion stars or circumstellar material provide the most reliable measurements of stellar masses. In the past two decades astronomers have applied several well-established techniques in order to measure dynamical masses of young stars, including analyzing eclipsing binaries, angularly resolved spectroscopic binaries, and young stars with circumstellar disks.

Table 1 presents dynamical mass measurements for 23 young ($t < 10$ Myr) stars with $M < 2 M_{\odot}$ (all the results of which we are aware at this writing). Column 2 presents the measured mass and uncertainty (random errors only; systematic uncertainties not included). Cols. 3 and 4 identify the dynamical technique used and the reference. Col. 5 gives the stellar radius for the EBs. Columns 6, 7, 8, and 9 list the spectral type when directly determined, effective temperature T_{eff} , luminosity, L , and the references for these quantities.

Mass measurements with accuracies better than 10% are necessary to begin to distinguish between the present suite of PMS evolutionary tracks. Table 1 shows that all the techniques can provide mass measurements of young stars with such a *precision* or better. However, each technique has unique limitations on its *accuracy*, which we briefly discuss in turn.

2.1 Techniques and Uncertainties

2.1.1 Eclipsing Binaries (EB). Eclipsing binaries are particularly valuable, for in addition to two mass measurements they can also provide direct measurements of the stellar radii and the ratio of the effective temperatures. As with most things valuable, PMS EBs are also rare, and to date only six have been discovered. Nonetheless, they provide 10 of the dynamical mass measurements in Table 1.

The eclipsing geometry by itself constrains the orbital inclination to be $\approx 90^{\circ}$, and with a standard light-curve analysis the inclination can be determined with a precision of $\sim 0.1\%$. In the case that the EB is also a double-lined spectroscopic binary (and indeed all of the PMS EBs discovered to date have been), the precision of the masses of both stars is then limited only by the precision of the double-lined orbit solution (i.e., by the number and precision of the radial velocity measurements). Importantly, at no point in the determination of the masses is the distance to the system required.

Subtle effects in the radial-velocity and light-curve analyses introduce systematic uncertainties. Radial velocities of double-lined systems are typically obtained via cross-correlation techniques that can produce systematic offsets in radial velocities of the

primary stars relative to their secondaries (e.g., *Rucinski* 1999). These effects can be minimized by selecting templates that are well-matched to the target stars in spectral type, by avoiding orbital phases subject to strong line blending, and by employing techniques designed either to accurately measure primary and secondary radial velocities when blended (e.g., TODCOR, *Zucker and Mazeh*, 1994) or fully disentangle the spectra of multiple components (e.g., *Simon et al.*, 1994, *Hadrava*, 1997). For the EBs listed in Table 1, where the radial-velocity amplitudes are large and blending of cross-correlation peaks is negligible over most of the orbit, these systematic errors in practice represent minor effects (i.e. $\sim 1\%$). For PMS stars a more significant effect is that of starspots, which introduce asymmetries in the line profiles and hence cause errors in the radial-velocity measurements that vary with the stellar rotation; such radial-velocity errors can be a few percent of the orbital semi-amplitudes. However, sophisticated light-curve analyses provide detailed information about spots that permit these effects to be well modeled in the orbit solution (e.g., *Stassun et al.*, 2004). Systematics in the light-curve analysis directly affect the masses only insofar as the determination of the inclination is concerned, the main uncertainty usually being the (wavelength-dependent) limb-darkening law. Again, in practice these systematic errors are minor (i.e. $< 1\%$).

Taking these systematic uncertainties into account, masses of PMS EBs have now been measured with accuracies of 1-2% (e.g., *Popper*, 1987; *Andersen*, 1991, *Stassun et al.*, 2004).

2.1.2 Astrometric/Spectroscopic Binaries (AS). Combination of relative astrometric and double-lined spectroscopic orbit solutions (AS) provides mass measurements for both stars, as well as a geometrical distance to the binary. (Both masses can also be derived from the combination of astrometric and single-lined spectroscopic orbit solutions if the distance is well known.) Until recently, studies of angularly resolved binaries (“Visual Binaries”; VBs) and spectroscopic binaries (SBs) have been entirely disconnected since the binaries detected as SBs had orbital separations that at the distance of star-forming regions fell far below the angular resolution limits of the available techniques. This situation has changed dramatically, first with application of the high-angular resolution capabilities of the Fine Guidance Sensors (FGS) of the *Hubble Space Telescope*, and now with adaptive optics (AO) at large telescopes and ground-based optical and infrared interferometers. Dynamical mass measurements of four stars from two AS systems are presented in Table 1. We anticipate that the summary table in the PPVI review will show a large increase in the number of AS binaries (Section 5).

The application of the AS technique to the two PMS binaries in Table 1 employed wholly or in part FGS data near instrumental angular resolution limits. As

such, systematic errors in the calibration are an important challenge that may propagate into the masses via the inclination angle i .

Looking to the very near future, new applications of the AS technique will rely in large part on interferometric data. The angular resolution limits of these observations are more than sufficient to achieve excellent mass-measurement precisions for PMS SBs in nearby star-forming regions. The limitations are that both components must "fit" within the beam of a single telescope, and that at least one star is bright enough for AO guiding and fringe tracking. These often are not the same thing because often the first is done in the visible and the second at the wavelength of observation.

If these limitations do not preclude an AS approach to a binary, then the primary concern is adequate orbital phase coverage, especially given the longer periods of the resolvable SBs in more distant star-forming regions. As these interferometric observations become more standard as a technique, both the time baselines and the number of measurements will increase and be less of a limitation. The photometric variability of PMS stars can also be a concern, particularly when the orbit solution is derived directly from visibilities.

Given present uncertainties in distance determinations, AS solutions are best achieved when the secondary star is detected spectroscopically; the resultant mass ratio makes a distance measurement unnecessary. Recently, detections of secondary spectra in PMS SBs have been greatly enhanced through near-infrared, high-resolution spectroscopy (*Steffen et al., 2001; Prato et al., 2002*).

2.1.3 Disk Rotation Curves (DK). The circumstellar disks around some young stars provide an additional method for measuring dynamical masses. When the disk mass is small compared to the star's mass (or, if a circumbinary disk, the binary mass), the disk rotation is Keplerian, and the amplitude of the rotation curve is determined by the mass of the star. Of course, the observed rotation curve must be corrected for inclination, which is typically derived from the morphology of the observed disk emission. Typically disk rotation curves have been observed via mm interferometry in CO lines (*Guilloteau and Dutrey, 1998; Simon et al., 2000*).

Measuring a mass with this technique requires knowing the linear radius in the disk at which a velocity is measured. Consequently, deriving a mass measurement requires a measured distance to the star. The uncertainty on the distance propagates linearly into the uncertainty on the mass. At present, the accuracies of distance measurements to individual young stars are generally poorer (e.g., of order 15% in Taurus-Auriga) than the internal precisions of the mass measurements. (Only the latter are given in Table 1.) *Simon et al. (2000)* reduce the effect of this systematic uncertainty in their tests of evolutionary models by doing the

comparison in the quantity L/M^2 . Since the luminosity L depends on the distance squared, this parameter is distance independent.

Additionally, the DK technique can be frustrated by line-of-sight molecular-line emission of the host molecular cloud at or near the systemic velocity of the disk. Of course, both the DK and AS techniques are useless if observations reveal that the targets are essentially face-on, or are unresolvable as disks or VBs.

2.2 Exemplars at the Forefront

Until ALMA comes on line in the next decade, we anticipate that most new mass measurements for young stars will derive from eclipsing binaries and angularly resolved spectroscopic binaries. With this in mind, we highlight here two recently studied systems that exemplify the capabilities and exciting scientific potential of applying these techniques to young stars.

The recently discovered Orion Nebula EB 2M0535-05 is a particularly important case study, for it comprises two young brown dwarfs (BDs; *Stassun et al., 2006*). With masses of $0.034 M_{\odot}$ and $0.054 M_{\odot}$, presently these stars alone constrain PMS stellar evolutionary theory below $0.3 M_{\odot}$.

Both the colors and spectra indicate that the primary BD has a spectral class of $M6.5 \pm 0.5$, or a surface temperature of $T_1 = 2650 \pm 100$ K (*Slesnick et al., 2004*). The measured temperature ratio of $T_2 / T_1 = 1.054 \pm 0.006$ implies a surface temperature for the secondary of $T_2 = 2790 \pm 105$ K. The luminosities of the BDs are calculated from the measured radii and surface temperatures, which when combined with the observed apparent magnitude and an appropriate bolometric correction yields a distance of 435 ± 55 parsecs, assuming no extinction. Extinction by as much as 0.75 visual magnitudes may be present, in which case the distance would be slightly smaller, 420 ± 55 parsecs. In either case the derived distance is in agreement with typical distances adopted for the Orion Nebula region (e.g., 480 ± 80 parsecs from *Genzel and Stutzki 1989*). Additional evidence for the association of 2M0535-05 with Orion is provided by its center-of-mass velocity, which is within 1 km s^{-1} of the systemic radial velocity of the Orion Nebula cluster.

The Orion Nebula star cluster is very young, with an age that has been estimated to be 1_{-1}^{+2} million years; thus *Stassun et al. (2006)* suggest a similar age for 2M0535-05. If any remaining disk material is coplanar with the binary (i.e., in an edge-on disk), the near-infrared colors of 2M0535-05 limit the amount of such material available for further accretion onto the BDs. The currently observed masses are therefore unlikely to change significantly over time; these BDs will forever remain BDs.

Encouragingly, the physical properties determined for the BDs in 2M0535-05 are broadly consistent with the most basic theoretical expectations.

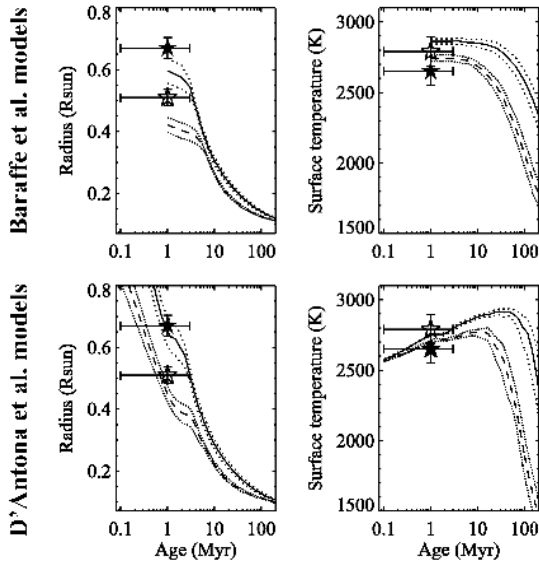


Figure 1: Comparison of the brown dwarf components of the eclipsing binary 2M0535-05 with evolution models of *Baraffe et al.* (1998) and *D'Antona and Mazzitelli* (1997).

The fact that 2M0535-05 comprises BDs that are both large and luminous—and even simply that they are of M spectral type—is a testament to the generally good predictive power of current theoretical models of young BDs. At the same time, there is a highly unexpected result in the ratio of their surface temperatures, $T_2 / T_1 = 1.054 \pm 0.006$; the less-massive BD is hotter than its higher-mass companion. Such a reversal of temperatures with mass is not predicted by standard theoretical models for coeval brown dwarfs, in which temperature increases monotonically with mass.

This result may be a clue to the formation history of brown dwarfs, if interpreted as evidence for non-coevality of the two BDs. Alternatively, the influence of magnetic fields and surface activity on convection may be affecting the energy flow in one or both stars. Or perhaps this result serves as yet another cautionary lesson on the difficulty of determining effective temperatures of very low-mass PMS objects. Improvement in atmosphere models and the subsequent calculation of spectral energy distributions may be required (see also Section 3.1.1). 2M0535-05 promises to serve as an important benchmark in our understanding of young brown dwarfs.

Many PMS mass measurements in the near future will derive from the application of optical/infrared interferometers coming on line to young spectroscopic binaries with existing and new orbit solutions. The first application of the AS technique to PMS stars was done by *Steffen et al.* (2001), who angularly resolved 045251+3016 with the FGS ($\rho < 0.05''$). The resultant astrometric orbital solution provided the inclination angle of the system, after which the masses were measured with precisions of 12%.

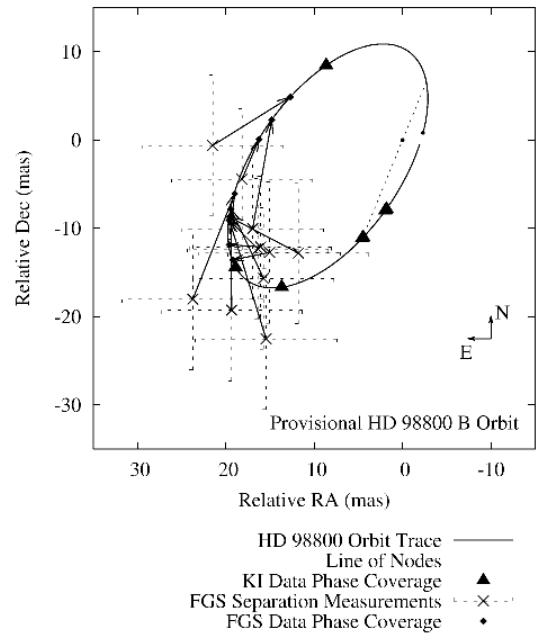


Figure 2: Astrometric data and orbit solution for HD98800 B (*Boden et al.*, 2005). Triangles are FGS measurements, circles are ground-based interferometry.

More recently, *Boden et al.* (2005) combined FGS data with ground-based K-band Keck interferometric visibility data to derive an astrometric orbital solution (Fig. 2) for HD 98800B, one binary in this PMS quadruple system. Notably, the filled circles in Fig. 2 do not represent separation measurements, but phases where Keck visibility data were obtained. These visibility functions were compared directly to model predictions in order to constrain the astrometric orbit, without an intermediate determination of separation.

Boden et al. (2005) find that the component masses, luminosities and effective temperatures of HD 98800B are inconsistent with solar-metallicity evolutionary tracks; they note that a lower metal abundance by a factor of 2-3 would resolve the discrepancy. Their study highlights a significant complication with the AS method, for even if a system is adequately resolved for orbital solutions it can be difficult to derive accurate stellar parameters, such as angularly resolved spectral energy distributions, by which to compare with theory. Careful analyses of the double-lined spectra are thus important.

This forefront observational study bodes well for a significant number of masses being measured via interferometry and spectroscopy in the very near future. Indeed, Haro 1-14c is under interferometric study and on the verge of yielding masses; the secondary is likely to have a mass $\approx 0.4 M_{\odot}$ (*Simon and Prato*, 2004; *Schaefer*, 2004). Ultimately, the lower-mass secondary stars in these binaries may prove the most valuable, as they provide tests of low-mass PMS evolutionary tracks.

3. COMPARISONS OF DYNAMICAL MASSES WITH PMS STELLAR EVOLUTION MODELS

3.1 Physical Properties of PMS Stars

The dynamically determined masses of PMS stars offer powerful tests of PMS stellar evolution models. However, conducting these tests requires not only accurate stellar mass measurements, but also accurately determined stellar properties, such as luminosities, effective temperatures, or radii, for comparisons with model predictions. For the 23 stars listed in Table 1, we have assembled the current best determinations of their stellar effective temperatures and luminosities; for the 10 stars in eclipsing systems, we also list their stellar radii. The methods by which these stellar properties have been determined merit some discussion.

3.1.1 Effective Temperature. About half of the effective temperatures presented in Table 1 have been derived via assigned spectral types. These spectral types are typically accurate to within 1 spectral subclass, which corresponds to approximately ± 150 K in effective temperature.

However, the uncertainty in the appropriate spectral type-temperature conversion scale at least doubles this uncertainty. Typically a dwarf-like temperature scale is assumed (e.g., *Legget et al.*, 1996), but slightly hotter temperature scales have been proposed for M-type PMS stars to account for their less-than-dwarf surface gravities (*White et al.*, 1999; *Luhman et al.*, 2003). Typically the proposed increase in temperatures is of order 100 K, but can become larger for the coolest stars. In Table 1, we use a temperature scale appropriate for dwarf stars (*Hillenbrand and White*, 2004).

Flux-calibrated spectral energy distributions (SEDs) or comparisons with synthetically generated spectra may provide the best determinations of effective temperature. This latter technique has been used for the case of BP Tau (*Johns-Krull et al.*, 1999), and bears real promise for future re-analyses of the binaries in Table 1.

For stars in EBs, analysis of the relative eclipse depths provides a very precise measure of the ratio of the stellar surface fluxes in the bandpass of the light curve, which in turn provides the *ratio* of effective temperatures via bolometric corrections from stellar atmospheres. EB effective temperature ratios are extremely precise, $< 1\%$. However, the accuracy of these effective temperature ratios is ultimately limited by the accuracy of the model atmospheres used in the light-curve synthesis. Finally, determining the effective temperatures for each star separately requires an external determination of the effective temperature of one of the stars, usually the primary. This determination is subject to the same uncertainties described above.

3.1.2 Radii. Direct measurements of PMS stellar radii are provided only by EBs. With well-sampled light curves, covering completely both eclipses (ingress and egress included), and additional information concerning the luminosity ratio (e.g., from spectroscopy in doubled-lined systems), the stellar radii (relative to the orbital semi-major axis) can be as precise as 1-2%. The effects of limb darkening complicate the analysis somewhat, but light curves at multiple wavelengths usually insure that these effects do not limit the accuracy of the measurements. Conversion to absolute radii requires accurate radial-velocity curves for both components. The median precision of the stellar radii measurements in Table 1 is 4%.

3.1.3 Luminosities. Luminosities are typically derived from a broad-band photometric measurement combined with an extinction correction (uncertainty of order 20% in the optical), a bolometric correction (uncertainty of less than 10%, except for the latest-type PMS stars), and a distance measurement. While a direct measure of the distance is provided for double-lined binaries with an AS solution, distances for the remaining stars are typically taken as those of their associated star-forming regions. Uncertainties in such distances, and in the location along the line of sight within the association, yield luminosity uncertainties as large as $\sim 40\%$.

For the stars in EBs, the individual luminosities are determined directly from the temperatures and radii via Stefan's law ($L = 4\pi R^2 \sigma T_{\text{eff}}^4$). For the 10 stars in eclipsing systems, the median precision of the luminosities is 15%, driven almost entirely by uncertainties in the effective temperatures.

Finally, we note that with knowledge of bolometric and extinction corrections, EBs yield an independent distance determination. Such distance measurements can be used to control measures derived for other stellar parameters, or to provide additional information on the distances to star-forming regions.

3.1.4 Other uncertainties. In addition to these known uncertainties, other characteristics of young stars likely bias the determined stellar properties in ways that are difficult to account for. Stars which are still actively accreting show excess optical and ultraviolet emission (e.g., *Basri and Batalha*, 1990; *Hartigan et al.*, 1991) and excess infrared emission from warm circumstellar dust (e.g., *Strom et al.*, 1989). These additional sources of radiation can confuse determinations of both effective temperatures and luminosities. Additionally, young stars can generate magnetic fields and associated cool-temperature star spots covering a large fraction of the stellar surface. Such spots confuse spectral analyses, bolometric and reddening corrections, etc. in as yet poorly quantified ways. Finally, many EBs have been found to be members of triple systems (e.g., V1174 Ori and TY CrA). Disentangling the light from the third star adds additional complexity and uncertainty.

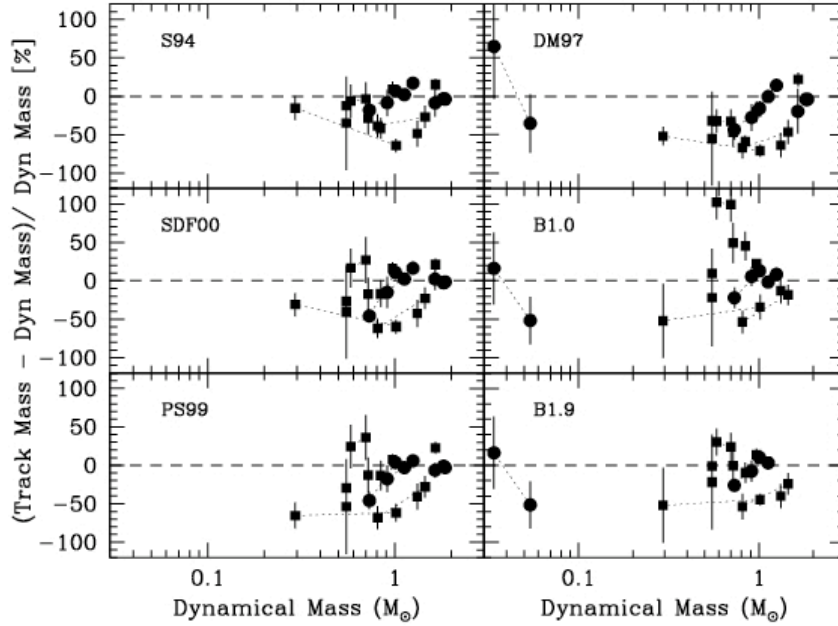


Figure 3: Percentage differences between theoretically and dynamically determined stellar masses versus dynamical stellar mass. *Circles* are components of eclipsing systems and *squares* are not. Error bars indicate only the random uncertainties in both the dynamical and theoretical masses.

These issues are particularly well illustrated by considering the three stars UZ Tau Ea, V1174 Ori B, and DM Tau. While these three stars are reported in the literature to have identical effective temperatures and luminosities that are the same to within 0.5 dex, their dynamically determined masses differ widely — $1.016 \pm 0.065 M_{\odot}$, $0.731 \pm 0.008 M_{\odot}$, and $0.55 \pm 0.03 M_{\odot}$, respectively. If the random uncertainties in the dynamical masses are reasonably assessed, then the inferred stellar properties must be in error. (Note that the uncertainty in distance has not been incorporated in the uncertainty for DM Tau.)

Cognizant of these uncertainties, we proceed to compare theoretical masses to dynamical mass measurements in order to test the success of theoretical PMS stellar evolution models. We follow the procedure of *Hillenbrand and White* (2004), who previously performed such a comparison for 17 of the 23 stars listed in Table 1, and add comparisons for the 6 stars in binaries identified more recently (V1174 Ori, HD 98800B, and 2M0535-05).

3.2 Comparison of Dynamical and Theoretical Masses

We compare the dynamically determined masses with the predictions of 6 evolutionary models that are widely used by the community to describe the physical properties of young objects. These models include

Swenson et al. (1994, approximately the series F models; hereinafter S94; $0.15\text{--}5.00 M_{\odot}$); *D’Antona and Mazzitelli* 1997 (DM97; $0.017\text{--}3.00 M_{\odot}$); *Baraffe et al.* (1998, BCAH98; B1.0; $0.035\text{--}1.20 M_{\odot}$); BCAH98 (B1.9; $0.035\text{--}1.20 M_{\odot}$); *Palla and Stahler* (1999; PS99; $0.1\text{--}6.0 M_{\odot}$); and *Siess et al.* (2000; SDF00; $0.1\text{--}7.0 M_{\odot}$). The physics in these models are given in Section 4. The BCAH98 models B1.0 and B1.9 differ only in the values of the mixing length α , which are 1.0 and 1.9 respectively.

Fig. 3 shows the comparisons of the theoretical masses predicted by these evolutionary models with the dynamically determined masses. The uncertainties indicated by the error bars include random uncertainties in the dynamical masses, and the random uncertainties in effective temperatures and luminosities (Table 1) as propagated into the theoretical masses.

The comparison in Fig. 3 shows a consistent tendency for the measured dynamical masses to be higher than the theoretical masses. Above $1.02 M_{\odot}$ the *mean* differences are only of order 10% for each of the theoretical models. Indeed, all models predict PMS masses that are consistent in the mean with dynamically measured masses to better than 1.6σ .

Below $1.02 M_{\odot}$ the mean differences increase to $\approx 20\%$ for the S94, PS99 and SDF00 models, and to 43% for the DM97 models. These differences in the mean are significant at the 2.5σ or higher level and begin to suggest meaningful discrepancies between the observations and the models.

The notable exceptions are the two sets of BCAH98 models, which in the mean continue to predict masses consistent with dynamical values at the 10% level ($< 1.4 \sigma$) for these lower-mass stars.

Curiously, the B1.0 models produce a standard deviation about the mean of 51%, substantially larger than any other model (which are in the range of 20-30%). These standard deviations represent reasonable estimates for the uncertainties in mass determinations for any given PMS star.

Currently there is only one star, UZ Tau Eb, with a dynamical mass between the BD mass limit and $0.5 M_{\odot}$. The trend of low theoretical masses continues for this star, though the difference for each theoretical model is not statistically significant when UZ Tau Eb is considered as a single case.

Other results generally support these findings. In a study of double-lined spectroscopic binaries having precisely determined mass ratios, *Palla and Stahler* (2001) showed that their evolutionary models predict consistent mass ratios for a sample of PMS stars above $1 M_{\odot}$. Using high-dispersion IR spectroscopy, *Prato et al.* (2002) studied a sample of 4 low-mass-ratio binaries, with companion masses as low as $\sim 0.2 M_{\odot}$ (based on theoretical primary masses and a dynamical mass ratio). They found that models predicted mass ratios that, while statistically consistent, were systematically less than the dynamically determined ratio. This can be interpreted again as the models underpredicting masses in the subsolar regime of the secondary stars.

Finally, *Stassun et al.* (2006; Section 2.2) present the first dynamical mass estimates for 2 young BDs. These masses are an order of magnitude lower than previous dynamical measurements and constrain evolutionary models at the very uncertain low-mass end. The theoretical masses of BCAH98 and DM97 (the only sets of theoretical models which extend this cool) agree with the observed masses to within a factor of 2.

As pointed out by *Hillenbrand and White* (2004), a hotter temperature scale for young M dwarfs would systematically shift the PMS theoretical masses to larger values, and could reconcile these discrepancies at sub-solar masses. A uniform shift in temperature scale by 150 K for stars below $1 M_{\odot}$ would bring the S94, PS99 and SDF00 models into good agreement; the DM models require a shift closer to 500 K.

Since PMS stars have surface gravities intermediate between those of dwarfs and giants, they may have intermediate temperatures as well. For comparison, while M0 dwarfs and giants have similar temperatures, M4 giants are systematically warmer by ~ 500 K (e.g., *Perrin et al.*, 1998). *Luhman et al.* (2003) propose a specific intermediate temperature scale for stars cooler than spectral type M0; the values were chosen to produce coeval ages for the T Tauri quadruple GG Tauri and for members of the IC 348 cluster using the BCAH98 $\alpha = 1.9$ evolutionary models.

Application of the *Luhman et al.* (2003) temperature scale improves the agreement of dynamical

and theoretical masses for most models, but makes the theoretical masses of the BCAH98 $\alpha=1.0$ models 22% higher than the dynamical masses. However, all of these adjustments are within the 3σ range for the uncertainties on the means. As such, the case for a particular temperature scale is not yet compelling.

Alternatively, these comparisons may provide guidance for resolving questions about the physics of stellar evolution theory. Such issues are presented in detail in Section 4.

These comparisons only hint at the potential value of a large sample of dynamical mass measurements for testing both observational techniques and stellar evolution theory. Another key finding from Fig. 3 is that the scatter of the differences between theoretical and dynamical masses for individual stars is larger than can be explained by the assigned random uncertainties. This scatter is not reduced when considering only those stars with the most precise dynamical mass measurements.

As such, we suggest that this additional scatter derives primarily from errors in the determination of effective temperatures and luminosities. *Additional dynamical mass determinations in the mass range of $0.5-2.0 M_{\odot}$ will not greatly improve the constraints on evolutionary models until these uncertainties in determining stellar properties are resolved.* Thus the marginal levels of significance of the discrepancies discussed in this section will only be reduced with improved determination of the stellar properties that link each star to theoretical models of stellar evolution.

3.3 Comparison of Observation and Theory in the Mass-Radius Plane

The PMS EBs provide constraints on evolutionary models that are independent of many of the uncertainties in determining effective temperatures and luminosities. In addition to having very accurately determined dynamical masses, the eclipsing pairs offer a direct measure of the stellar radii. Thus comparison with theoretical models can be done in the mass-radius (M-R) plane, thereby preserving the accuracy of the measurements and avoiding issues related to uncertain temperature scales. Specifically, EBs allow tests of the mass-radius relationships of theoretical models, given an assumption of coevality for the pair of stars within each EB.

Three of the PMS EBs — 0529.4+0041 AB, V1174 Ori AB, and 2M0535 AB — consist of two PMS stars that are significantly different in mass and temperature. Such pairs offer the most interesting constraints on theoretical models since they span a broad range of predicted properties. Of these 3 systems, V1174 Ori has masses and radii determined with sufficient accuracy ($< 2\%$) to permit strong conclusions, and so we present this EB in some detail here.

In Fig. 4 V1174 Ori is compared in the M-R plane with the models of BCAH $\alpha = 1.9$ and PS $\alpha=1.5$.

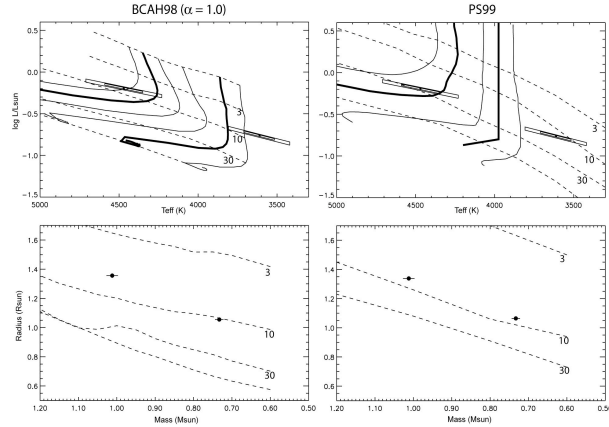


Figure 4: L - T_{eff} and mass-radius (M - R) plots comparing the measurements of the eclipsing binary V1174 Ori with the PMS models of BCAH98 ($\alpha=1.0$) (left) and PS99 (right). *Dashed lines* represent isochrones with ages in Myr as labeled. *Solid lines* represent mass tracks, with those appropriate to the dynamical masses ($1.01 M_{\odot}$ and $0.73 M_{\odot}$) emphasized. *Nested parallelograms* represent the 1- and 2- σ confidence intervals in T_{eff} and $\log L$. Note that the positions of the primary and secondary in these uncertainty domains are highly correlated, in the sense that a hotter primary is associated with a hotter secondary.

These models were selected to show the improved performance of models with lower convective efficiency, a general trend found by *Stassun et al.* (2004). For such models the current generation of PMS tracks is performing well in predicting the PMS mass-radius relationship — arguably two of the most fundamental physical parameters of young stars. This agreement may indicate that the equations of state in the theoretical models are accurate (see also the discussion in Section 4.4.6). Importantly, though, different theoretical models still yield different ages.

Interestingly, success of models in the M - R plane does not necessarily translate to success in the T_{eff} - L plane. The PS99 models yield isochrones parallel to the observed M - R relationship, yet fail to simultaneously yield coevality in the T_{eff} - L plane. Even more strikingly, while both sets of tracks can match the T_{eff} - L position of the $1.01 M_{\odot}$ primary at the 2σ level or better, they fail miserably at simultaneously matching the T_{eff} - L position of the $0.73 M_{\odot}$ secondary. For example, the PS99 mass tracks corresponding to the secondary mass are 500 K too warm.

Similar analyses (and results) are done for a suite of current models by *Stassun et al.* (2004). Importantly, the accurate temperature ratio for V1174 clarifies that a simple shift in the temperature scale cannot resolve the discrepancies for all models. The mass tracks are too compressed in effective temperature to ever simultaneously fit the locations of these stars.

3.4 Lithium as a Test of PMS Evolution Models

While these tests of PMS models focus either on global physical properties (e.g., mass, radius) or on surface properties (e.g., effective temperature, luminosity), the predicted evolution of abundances (e.g., lithium and deuterium) may provide a powerful probe of PMS stellar interiors, particularly with respect to convection. *Stassun et al.* (2004) examined the Li abundances of all PMS stars with dynamical mass determinations (Fig. 5) and were able to draw several conclusions. First, the observed pattern of increased Li depletion with decreasing mass is, qualitatively, as predicted; the deeper convective zones of cooler stars, over this mass range, lead to more efficient depletion. More quantitatively, the absolute level of depletion observed again favors models with inefficient convective mixing. For example, the observed Li depletion for the components of V1174 Ori agrees well with the BCAH98 $\alpha=1.0$ models, while these models with $\alpha=1.9$ predict at least two orders of magnitude greater depletion than observed in the secondary.

The Li data again reveal likely problems with the determination of stellar parameters. For example, the observed Li depletion of DL Tau is an order of magnitude too low for its mass. This same star is discordant in terms of its placement in the H-R diagram relative to other stars of similar empirical mass; the $0.73 M_{\odot}$ secondary of V1174 Ori is 450 K cooler than the inferred temperature for DL Tau, even though their masses are nearly identical. Possibly these discrepancies may be tied to DL Tau being one of the most actively accreting stars in the sample.

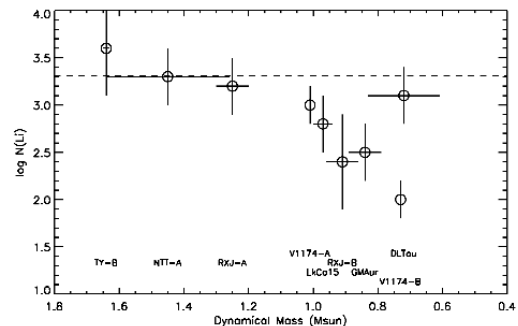


Figure 5: Li abundances for all PMS stars with dynamical mass determinations and Li abundance measurements in the literature. The cosmic abundance is represented by the horizontal dashed line.

4. THEORETICAL MODELS OF PMS STELLAR EVOLUTION

The comparisons discussed in the previous section suggest interesting discrepancies between

observations and theoretical models at young ages, and specifically possible systematic underestimates of theoretically predicted masses. Unfortunately, the uncertainties in these theoretical masses resulting from uncertainties in the stellar properties do not yet permit unambiguous tests of PMS evolutionary models. With the recent increase in the number of dynamical mass measurements, the reduction of these uncertainties must be a critical objective for progress in the field. In parallel, it is important to identify the key physical uncertainties affecting the theory, and to assess whether the mass comparisons might provide guidance for improvement of the theory.

Important progress has been made within the past few years regarding the theory of very-low-mass stars (VLMS; $M < 1 M_{\odot}$) and BDs ($M < 0.075 M_{\odot}$). The main improvements concern the equation of state (EOS) of dense plasmas and the modeling of cool, dense atmospheres. These theoretical efforts have yielded both a better understanding of these objects and good agreement with observations of older objects (age $\gg 10$ Myr).

Although several shortcomings remain (as discussed in Section 4.4), the improved reliability of the current theory for VLMS and BDs allows us to return to a thorough analysis of theoretical models of young objects. From the theoretical viewpoint, young objects represent a formidable challenge given the extra level of complexity from processes such as accretion, rapid rotation, and magnetic activity that are characteristic of the early phases of stellar evolution.

4.1 Physics of Low-Mass Stars and Brown Dwarfs

One of the main theoretical achievements of the past years in the modeling of VLMS concerns the description of their thermodynamic properties. VLMS and BDs are dense, cool objects, with typical central densities of the order of $100 - 1000 \text{ gm cm}^{-3}$ and central temperatures lower than 10^7 K . Under such conditions, a correct EOS for the description of their inner structure must take into account strong interactions between particles, resulting in important departures from a perfect gas EOS (cf. *Chabrier and Baraffe, 1997*). Important progress has been made by *Saumon et al. (1995)* who developed an EOS specifically designed for VLMS, BDs, and giant planets. Since the EOS determines the mechanical structure of these objects, and thus the mass-radius relationship, it can be tested against direct observations of stellar radii obtained via EBs, planetary transits, or interferometric measurement. Also, several high-pressure shock wave experiments have been conducted in order to probe the EOS of deuterium under conditions characteristic of the interior of these objects. The Saumon-Chabrier-VanHorn EOS was found to adequately reproduce the experimental pressure-density profiles of gas gun shock compression experiments at pressures below 1 Mbar, probing the domain of molecular hydrogen dissociation. However, discrepancies were found with the experimental temperatures. Recent experiments at higher pressure, testing the domain of pressure-ionization ($P \sim 1\text{-}3$ Mbar), unfortunately give results different from the Saumon-Chabrier-VanHorn EOS. Robust comparisons between experiments and theory in this critical pressure regime cannot be done before this discrepancy is resolved.

Table 2: Input Physics in Current Theoretical PMS Stellar Evolution Models

Authors	EOS	Atmosphere	Convection	I_{mix}/H_p
B97	SCVH	Grey atmosphere: solve RT equation	MLT	1.5
BCAH98	SCVH	Non-grey atmosphere: NextGen	MLT	1.0; 1.9
DM94	<i>Magni and Mazzitelli 1979</i>	Grey approx: $T(\tau)$ relationship	MLT CM	1.2
DM97	<i>Magni and Mazzitelli 1979</i>	Grey approx: $T(\tau)$ relationship	CM	
PS99	<i>Pols et al. 1995</i>	Grey approx: $T(\tau)$ relationship	MLT	1.5
SDF00	<i>Pols et al. 1995</i>	Non-grey atmosphere: Uppsala models (Plez)	MLT	1.6
S94	<i>Eggleton et al. 1973</i>	Grey approx: $T(\tau)$ relationship	MLT	1.957

Another essential physical ingredient for theoretical models of VLMS and BDs concerns atmosphere models. VLMS are characterized by effective temperatures from 5000 K down to 2000 K and surface gravities of $\log g \sim 3 - 5.5$, while BDs cover a much cooler temperature regime extending down to 100 K. (Young BDs, however, remain relatively hot, with temperatures in excess of 2000 K.)

Such effective temperatures allow the presence of stable molecules, in particular metal oxides and hydrides (TiO, VO, FeH, CaH, MgH) which are the major absorbers in the optical, and CO and H₂O which dominate in the infrared. These molecules cause strong non-grey effects and significant departures of the spectral energy distribution from black body emission. Another difficulty inherent in cool dwarf atmospheres is the presence of convection in the optically thin layers. This is due to the molecular hydrogen recombination ($H+H \rightarrow H_2$), which lowers the adiabatic gradient and favors the onset of convective instability.

Since radiative equilibrium is no longer satisfied in such atmospheres, the usual procedure of imposing outer boundary conditions based on standard $T(\tau)$ relationships from grey atmosphere models is incorrect. *Chabrier and Baraffe* (1997, 2000) show that as soon as molecules form in the atmosphere (i.e for $T_{\text{eff}} \leq 4000$ K), the use of standard $T(\tau)$ relationships and grey outer boundary conditions, like the well known Eddington approximation, overestimates the effective temperature for a given mass and yields a higher hydrogen-burning minimum mass. An accurate surface boundary condition based on non-grey atmosphere models is therefore required for evolutionary models.

4.2 PMS Evolutionary Models

Various sets of tracks can be found in the literature, and detailed comparisons are given by *Siess et al.* (2000) and *Baraffe et al.* (2002). Here we briefly comment on the main input physics of the models used in the analyses of Section 3. Table 2 summarizes the key physical inputs in each model. Only the BCAH98 and the SDF00 models use non-grey atmosphere models for outer boundary conditions. *D'Antona and Mazzitelli* (1994, DM94), DM97 and PS99 use approximate boundary conditions based on $T(\tau)$ relationships assuming a grey approximation and radiative equilibrium. Consequently, for a similar treatment of convection, the DM94 models for VLMS are usually hotter than the BCAH98 models. The *Burrows et al.* (1997, B97) models for VLMS and hot BDs ($T_{\text{eff}} > 2000$ K) are based on grey atmosphere models obtained by solving the radiative transfer equation. Such an approximation, although it represents an improvement over the previous $T(\tau)$ relationships, still overestimates effective temperature at a given mass compared to evolution models based on full non-grey atmospheres.

Above 4000 K, the choice of the outer

boundary condition (BC) has less influence and the treatment of convection becomes more crucial. Convection in most of the models is treated within the framework of the mixing length theory (MLT), with a mixing length $1 < l_{\text{mix}} < 2$. Only DM94 and DM97 differ by using the Canuto-Mazzitelli (CM) formalism.

The treatment of convection affects the temperature gradient in convective zones. In solar-type stars, above $T_{\text{eff}} \sim 4000$ K, it affects primarily the radius of an object, and to a lesser extent its luminosity. For such objects, an increase in the mixing length yields a decrease of the radius (for a given mass at a given age) and thus an increase of the effective temperature, shifting Hayashi lines toward hotter effective temperature (see *Baraffe et al.*, 2002 for a discussion). This is why the DM97 Hayashi lines behave differently with respect to models of other groups, as noted by SDF00. The Canuto-Mazzitelli treatment of convection yields results at odds with 3D hydrodynamic simulations for the outer thermal profile of the Sun (see e.g., *Nordlund and Stein*, 1999), and does not provide an accurate treatment of convection in optically thin media, at least for solar-type stars and low-mass stars (see e.g., *Chabrier and Baraffe*, 2000).

As a last remark, we note that the comparison of observations with evolutionary models based on BCs provided by non-grey atmosphere models are much more instructive, since it confronts *both* the inner atmosphere profile (which determines the BC and fixes the M- T_{eff} and M-L relationship) and the outer atmosphere profile and resultant spectral synthesis (through synthetic spectra and colors).

4.3 Successes of the Theory

Before applying current theory to the complex case of young objects, it is essential to confront first the more accessible and accurate observations of old VLMS and BDs. Several successes of the theory, including color-magnitude diagrams of globular clusters, mass-magnitude and mass-radius relationships, and near-IR color-magnitude diagrams for open clusters (see *Chabrier et al.*, 2006 and references therein), tell us that uncertainties due to the input physics have been considerably reduced. Fig. 6 displays a comparison between observed and predicted mass-radius relationships and shows the good agreement with observations. This agreement is achieved down to the very bottom of the main sequence with the recent observation of the smallest H-burning object known (*Pont et al.*, 2005). The same theory applied to giant planets, where the description of pressure ionization and H₂ dissociation is even more crucial, also provides excellent agreement with measured radii of exoplanet transits (*Baraffe et al.*, 2005). This gives confidence in the underlying physics describing the mechanical structure of low-mass objects. The general description of spectral properties of M-dwarfs is also satisfactory, although with some problems to be discussed below.

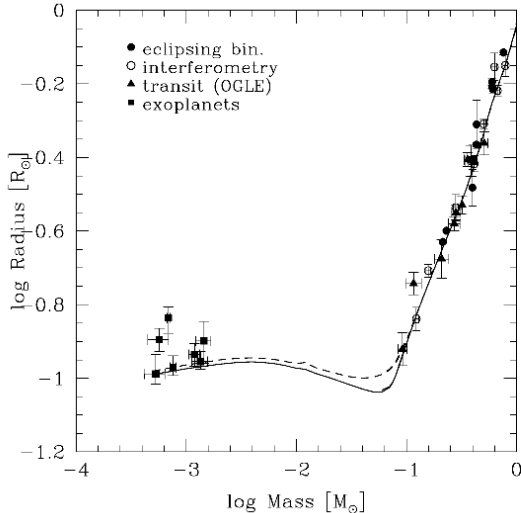


Figure 6: Observed and theoretical mass – radius relationships. Observations are compared to the models of BCAH98 for different ages (0.5 Gyr (dashed curve) and 1 Gyr (solid curve)).

4.4 Failures of the Theory

Although current models for VLMS and BDs provide generally good agreement with observations, several shortcomings remain. In this subsection we describe some of the known failings of the models. In the next subsection we discuss possible explanations and improvements that are still required in various domains.

(i) A shortcoming pointed out in BCAH98 concerns the optical colors (V-I) and (R-I) for solar metallicity models. These are significantly too blue for objects fainter than $M_V \sim 10$.

(ii) In the near-IR, current atmosphere models, based on the most updated molecular line lists, do not provide satisfactory agreement with observed color-magnitude diagrams (see *Allard et al., 2000* for discussion).

(iii) A discrepancy between observed and theoretical radii of EBs with low mass components ($M < 1 M_\odot$) has been pointed out for several systems (see *Torres et al., 2006* and references therein). The predicted values are usually 10%-15% smaller than observed.

(iv) Recent observations of young binary systems suggest a problem in the mass-luminosity relationship of young low-mass objects (*Close et al., 2005; Reiners et al., 2005*), in the same sense as found by *Hillenbrand and White (2004)* and discussed in Section 3. These observations and their interpretation are still controversial, especially with respect to AB Dor (*Luhman and Potter, 2006; Luhman et al., 2005*).

(v) *Mohanty et al. (2004a,b)* pointed out a problem in the spectroscopic analysis of young, low-gravity objects. Comparing observed and synthetic spectra, they use molecular bands of TiO and lines of neutral atomic alkalis to determine the effective temperatures and surface gravities of M-type PMS objects. They find gravities that are not in agreement with predictions from evolutionary models for the coolest objects and argue that uncertainties in the models may be responsible for this discrepancy.

(vi) A discrepancy between the age derived from lithium depletion and the age derived from isochrones has been recently pointed out for young systems (*Song et al., 2002; White and Hillenbrand, 2005*).

(vii) Finally, we note that there remain as yet unquantified theoretical uncertainties in the accuracies of theoretical spectra. Synthetic spectra are typically only tested through reference to the solar spectrum (e.g., *Johns-Krull et al., 1999*). These uncertainties also propagate into theoretical spectral energy distributions, from which bolometric corrections are derived.

4.5 Physical Issues

Among this list of discrepancies between observations and models, the problems (i)-(iii) are robust and clearly indicate problems with our current modeling of low-mass objects. The other points (iv)-(vi) are to be taken with caution and must await confirmation. The conclusions reached by the studies mentioned in (iv)-(vi) depend strongly on details of the observational analyses that are not yet secure. Finally, point (vii) requires improvement of synthetic spectra in order to quantify current uncertainties.

Here we consider the key physical issues that might lead to resolution of these discrepancies between observation and theory.

4.5.1 Molecular opacities. The problems mentioned in (i) and (ii) concerning shortcomings in optical colors and near-IR colors/spectra point to still inaccurate molecular linelists. The linelists and/or oscillator strengths of TiO and H₂O, which are important absorbers in the optical and the near-IR respectively, are still imperfect. This may not only affect the colors and spectra, but may also bear consequences for the atmospheric structure and thus on the evolutionary properties (e.g., luminosity and effective temperature versus mass and age).

The introduction in current atmosphere models of the AMES-TiO linelist reduces the mismatch in optical colors found in BCAH98, but still not to a satisfactory level (*Allard et al., 2000; Chabrier et al., 2000*). This seems to point to remaining uncertainties in TiO opacities. Also, the treatment of the opacities for

MgH, CaH, CrH, FeH and VO is still uncertain in current atmosphere models, affecting spectroscopic analysis in the optical (F. Allard, priv. comm). These uncertainties must be remembered especially when performing spectroscopic analyses based on TiO lines. Because of these uncertainties, the gravities and effective temperatures derived by *Mohanty et al.* (2004a, b) are to be taken with caution.

With respect to water, an important source of opacity affecting both SEDs and thermal atmosphere profiles, the most recent linelists available still provide an unsatisfactory agreement with observed spectra of M-dwarfs (see *Allard et al.*, 2000 and *Jones et al.*, 2002 for details) and with color-magnitude diagrams in the near-IR (see e.g., Fig. 6 of *Chabrier et al.*, 2000).

4.5.2 Line broadening. Under density and pressure conditions characteristic of cool atmospheres, the treatment of spectral line broadening provides another source of uncertainties. We stress that these uncertainties may affect spectroscopic analyses devoted to the determination of fundamental parameters (gravity, effective temperature) from line profile fitting. This may be another explanation for the discrepancy pointed out in the *Mohanty et al.* analysis. Theoretical efforts are now being devoted to the modelling of absorption profiles perturbed by He and molecular H₂, a complex fundamental problem in physics (*Allard et al.*, 2005). Such theoretical improvement will hopefully reduce the uncertainties due to the treatment of collisional line broadening in the next generation of atmosphere models.

4.5.3 Convection. The treatment of convection is known to be an important source of uncertainty in the evolution of stars with masses $M > 0.6 M_{\odot}$ at any age (see *Chabrier and Baraffe*, 2000; *Baraffe et al.*, 2002). The effect of a variation of the mixing length l_{mix} , used in the Mixing Length Theory (MLT), on evolutionary tracks for solar-type stars is well known and is illustrated for example in Fig. 2b of *Baraffe et al.* (2001).

For masses $M < 0.6 M_{\odot}$, the super-adiabatic layers retract appreciably and the transition from convective to radiative outer layers is characterized by an abrupt transition from a fully adiabatic to a radiative structure with a very small entropy jump. This means that during most of the evolution, *except at early ages* (see below), the sensitivity of the evolutionary models to l_{mix} is small for this mass range. Multi-dimensional hydrodynamical simulations for conditions characteristic of M-dwarf atmospheres, $T_{\text{eff}} \leq 3000$ K, $\log g = 5$, have been conducted by *Ludwig et al.* (2002). These simulations confirm the aforementioned small entropy jump found in the 1D models described by MLT, illustrating the large efficiency of atmospheric convection for these objects due to the formation of molecules. Under these circumstances, the 3D

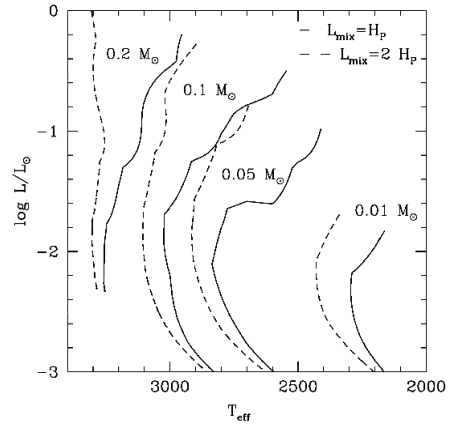


Figure 7: Effect of the mixing length parameter on evolutionary tracks of VLMS and BDs (*Baraffe et al.*, 2002)

simulations show that MLT does indeed provide a correct thermal profile, providing a value of $l_{\text{mix}} > H_p$ (with H_p a pressure scale height), at least for high gravities ($\log g > 4$) and older objects ($t \gg 10$ Myr).

As emphasized in *Baraffe et al.* (2002) and shown in Fig. 7, the evolution of very young objects with $M < 0.6 M_{\odot}$ and gravities $\log g < 4$ can be affected by the treatment of convection. *Ludwig et al.* (2006) extended their 3D numerical simulations of convection to atmosphere models with gravities of $\log g < 4$, i.e. appropriate for PMS stars and young BDs. They find values of $l_{\text{mix}} \sim 2 H_p$ to match the entropy of the deep regions of the convective envelope, whereas a larger value of l_{mix} , between $2.5 H_p$ and $3 H_p$, is required to match the thermal structure of the deep photosphere (*Ludwig et al.* 2006). This means that current spectral analysis of PMS objects and young BDs based on MLT atmosphere models calculated with $l_{\text{mix}} = 2 H_p$ could significantly overestimate the effective temperature. Work is currently under way to determine a better calibration of l_{mix} in such low gravity atmosphere models in order to reduce the uncertainties on the thermal profile in the deep interior, which may affect the evolutionary properties at young ages, and in the outer layers, where the spectrum emerges.

4.5.4 Accretion. Accretion is an important process that may affect the early phase of evolution of stars and brown dwarfs. Signatures of accretion onto young objects are now observed over a wide range of masses down to the substellar regime.

In the VLMS and BD regime observed accretion rates for ages greater than 1 Myr are rather low, ranging from $5 \times 10^{-9} M_{\odot} \text{ yr}^{-1}$ to $\sim 10^{-12} M_{\odot} \text{ yr}^{-1}$, with a sharp decrease of the rate with mass (roughly proportional to M^2 ; *Mohanty et al.*, 2005 and references therein). Theoretical and observational arguments suggest that accretion rates increase with younger age so that rates are significantly larger at ages earlier than 1

Myr (Henriksen *et al.*, 1997; Mohanty *et al.*, 2005).

The effects of accretion on the structure and evolution of young stars have been widely investigated since the seminal work by *Stahler* (1988), and a summary can be found in the chapter by *Chabrier et al.* Here we only briefly discuss the main effects.

As shown by *Hartmann et al.* (1997) assuming that most of the thermal energy released by accretion is radiated away instead of being added to the stellar interior, accreting low-mass stars are expected to be more compact than their non-accreting counterparts with same mass and same age. Consequently, an accreting object looks older in a L - T_{eff} diagram than a non-accreting object of same mass and age. Thus, ages assigned from non-accreting tracks can be overestimates. Effects can be even more drastic if a non-negligible fraction of the thermal energy from the accretion shock is transferred to the interior. Several authors have investigated such possibilities (see the chapter of *Chabrier et al.* and references therein) and found that convection could be inhibited, with profound modifications on the stellar structure. The amount of thermal energy released from accretion and added to the stellar interior is poorly known, since it depends highly on the details of the accretion mechanisms and the properties of the accretion shock.

4.5.5. Initial conditions Most low-mass PMS models available in the literature, including those considered here, start from arbitrary initial conditions that are totally independent of the outcome of the prior protostellar collapse and accretion phases. The initial configuration is a fully convective object starting its contraction along the Hayashi line from arbitrarily large radii. Evolution starts prior to or at central deuterium ignition, with initial central temperatures $\sim 5 \times 10^5$ K.

According to studies of the protostellar collapse and accretion phases, such initial conditions are oversimplified and low-mass objects could form with significantly smaller radii (*Hartmann et al.* 1997 and references therein). *Baraffe et al.* (2002) demonstrated the arbitrariness of current initial conditions and starting times for evolutionary tracks, and emphasized the large uncertainty in assigning ages to objects younger than a few Myr based on current PMS tracks.

To resolve these substantial uncertainties requires self-consistent evolution from the 3D protostellar collapse phase to the subsequent PMS evolution, a significant theoretical challenge in the field of star formation and evolution.

4.5.6 Magnetic activity. Understanding the effects of magnetic activity, usually linked to rapid rotation, on the inner structure and atmosphere of low-mass objects is still far from reach (*Chabrier and Kueker*, 2006). However there are suggestions about the nature of these effects and their possible importance. As an

example, the discrepancy of 10%-15% found between observed and predicted radii of some main-sequence EBs may be related to the magnetic activity of the components. This idea arises from the fact that inactive stars agree well with model predictions, whereas the most active ones appear systematically too large (see e.g. *Torres et al.*, 2006). The inhibition of convective heat transport due to strong magnetic fields and/or the presence of numerous spots on the stellar surface could be responsible for such structural changes.

If such effects are confirmed, the constraints provided by the EB mass-radius relationship on current PMS evolutionary models that do not account for these effects may be limited. We even speculate that the agreement mentioned in section 3.3. between the observed M-R relationship and current generations of may be fortuitous. The discrepancy between data and models in the T_{eff} - L plane shown in Fig. 5, in opposite to the good agreement found in the M-R plane, reveals the existence of remaining problems.

A quantitative estimate of such effects is a difficult task. Modelers have begun to explore them (e.g. *Ventura et al.*, 1998, *Mullan and MacDonald*, 2001), but their treatments remain very simplified. The huge progress of multi-dimensional magnetohydrodynamic simulations expected in the near future will definitely improve our understanding of these effects.

Another effect related to magnetic activity concerns the formation of lithium lines. Lithium abundance analysis in the presence of strong chromospheres should be taken with caution. As suggested by *Pavlenko et al.* (1995), Li I lines may be significantly affected by the presence of a chromosphere, which could reduce their strength. Such an effect would thus yield an incorrect determination of the level of Li depletion in young objects. This could explain the discrepancies mentioned in Section 3 between V1174 Ori and DL Tau. A systematic search for possible correlations between the level of lithium depletion and the level of H_{α} emission (as one measure of chromospheric strength) may provide some clues to address this problem.

4.6 Final Remarks

In the previous sections, we have tried to highlight the challenges and new problems that theorists and observers are facing when analyzing young stars. Theorists are working hard to resolve the physical issues listed above. But at the time this review is being written, we are not able to estimate their quantitative effects on observable quantities.

Looking to the future, rapid progress is expected with respect to opacities and convection. But improving our knowledge of initial conditions and of magnetic activity is a major challenge for the future.

5. VISIONS OF THE FUTURE

Of the 23 masses listed in Table 1, 20 have been contributed since the 1998 meeting of *Protostars and Planets!* Both the greater availability of classical instrumentation and powerful innovative facilities now being built suggest that future progress will be at least as rapid. The capability to measure masses precisely over more than a decade of stellar mass will continue to be driven by technological developments. The number of PMS EBs is being increased by extensive photometric surveys enabled by large format detectors at modest-aperture telescopes. It has proven difficult to apply the DK technique to young stars estimated to have stellar masses less than $0.5 M_{\odot}$ because the CO emission of their disks is weak (Schaefer, 2004). ALMA may be expected to advance this technique through its sensitivity and its access to a new and very large sample of young star targets in the southern sky. The development of multi-baseline IR interferometers such as VLTI, KI, and CHARA will enable the measurement of astrometric orbits of a large sample of SBs. Similarly, the advent of laser-guided AO removes the limitation that the young star targets, often in dark clouds, be located near suitable "natural" guide stars. The integral-field high-resolution IR spectrographs now planned will speed the identification of SB2s with low-mass secondary stars in compact clusters. And in the more distant future, astrometric space missions will provide distance estimates of remarkable accuracy for young stars, converting relative astrometric orbits and rotation curves into accurate masses. The most important products of this variety of techniques will be dynamical mass measurements for stars below $0.5 M_{\odot}$.

While mass is the fundamental stellar parameter, it is not the only parameter necessary for a comparison with theoretical stellar evolution models. For each star we also need a combination of luminosity, effective temperature, and radius. A promising route to effective temperatures is detailed comparison of high-dispersion spectra with synthetic spectra. As an example, the temperature of the young T Tauri stars Hubble 4 and TW Hydrae have been determined with precisions of 56 K and 24 K, respectively (Johns-Krull et al., 2004; Yang et al., 2005). In addition, this analysis permits precise determination of any excess continuum emission caused by accretion and metallicity ($[M/H] = -0.08 \pm 0.05$, in the case of Hubble 4), both of which can bias luminosity and temperature estimates.

Recent advances in atmosphere models and more complete molecular opacity tables now allow codes to produce synthetic spectra that agree remarkably well with those of young stars, even at very low masses. In principle, such analyses can allow for a direct determination of both stellar temperature and surface gravity. Our description of the remaining uncertainties on opacities, line broadening, and convection suggests that present atmosphere models

may not yet provide very accurate measures. Still, the early successes auger well for this approach.

Finally, for the young stars that are surprisingly nearby — as close as 20 pc (Zuckerman and Song, 2004) — interferometric measurements of their diameters may enable astronomers to directly measure the radii of stars not in EBs (Simon, 2006).

The essential message of this review is that with the acquisition of larger numbers of dynamical mass measurements for PMS stars, the limitation in testing stellar evolution theory via stellar masses has become the determination of comparably accurate theoretical mass predictions for these same stars. We suggest that presently the limitation is primarily in the measurement of effective temperatures and luminosities. We emphasize that there are immediately realizable prospects for improving effective temperature and luminosity measurements for young stars. Thus we urge the community to apply itself to the determination of much improved theoretical masses for the 23 stars with measured dynamical masses.

Acknowledgements The authors would like to thank the very constructive review of the referee Luiz Paulo Vaz. The United States authors would like to gratefully acknowledge funding support from the U.S. National Science Foundation.

References

- Allard N., Allard F., and Kielkopf J. F. (2005) *Astron. Astrophys.*, 440, 1195-1201.
- Allard F., Hauschildt P. H., and Schwenke D. (2000) *Astrophys. J.*, 540, 1005-1015.
- Andersen J. (1991) *Astron. Astrophys. Rev.*, 3, 91-126 (A91)
- Baraffe I., Chabrier G., Allard F., and Hauschildt P. H. (1998) *Astron. Astrophys.*, 337, 403-412 (BCAH98).
- Baraffe I., Chabrier G., Allard F., and Hauschildt P. H. (2001), In *From Darkness to Light: Origin and Evolution of Young Stellar Clusters* (T. Montmerle and P. André, eds.), pp. 571-580. ASP Conference Series, v. 243, San Francisco.
- Baraffe I., Chabrier G., Allard F., and Hauschildt P. H. (2002) *Astron. Astrophys.*, 381, 563-572 (BCAH02).
- Baraffe I., Chabrier G., Barman T. S., Selsis F., Allard F., and Hauschildt P. H. (2005) *Astron. Astrophys.*, 436, L47-L51.
- Basri G. and Batalha C. (1990) *Astrophys. J.*, 363, 654-669.
- Boden A. F., Sargent A. I., Akeson R. L., Carpenter J. M., Torres G., et al. (2005) *Astrophys. J.*, 635, 442-451 (B05).
- Burrows A., Marley M., Hubbard W. B., Lunine J. I., Guillot T., et al. (1997) *Astrophys. J.*, 491, 856-875.
- Casey B. W., Mathieu R.D., Vaz L. P. R., Andersen J., and Suntzeff N. B. (1998) *Astron. J.*, 115, 1617-1633 (C98).
- Chabrier G. and Baraffe I. (1997) *Astron. Astrophys.*, 327, 1039-1053.
- Chabrier G. and Baraffe I. (2000) *Ann. Rev. Astron. Astrophys.*, 38, 337-377.
- Chabrier G., Baraffe, I., Allard F., and Hauschildt P. H. (2000)

- Astrophys. J.*, 542, 464-472.
- Chabrier G. and Kueker M. (2006) *Astron. Astrophys.*, 446, 1027-1038
- Close L., Lenzen R., Guirado J. C., Nielsen E. L., Mamajek E. E., et al. (2005) *Nature*, 433, 286-289.
- Covino E., Catalano S., Frasca A., Marilli E., Fernández M., et al. (2000) *Astron. Astrophys.*, 361, L49-L52 (C00).
- D'Antona F. and Mazzitelli I. (1994) *Astrophys. J. Suppl.*, 90, 467-500 (DM94).
- D'Antona, F. and Mazzitelli, I. (1997) *Mem. della Soc. Astron. Ital.*, 68, 807-822 (DM97).
- Dutrey A., Guilloteau S., and Simon M. (2003) *Astron. Astrophys.*, 402, 1003-1011 (D03).
- Eggleton P. P., Faulkner J. and Flannery B. P. (1973), *Astron. Astrophys.*, 23, 325-330.
- Genzel R., and Stutzki J. (1989) *Ann. Rev. Astron. Astrophys.*, 27, 41-85.
- Guilloteau S. and Dutrey A. (1998) *Astron. Astrophys.*, 339, 467-476.
- Hadrava P. (1997) *Astron. Astrophys. Suppl.*, 122, 581-584.
- Hartigan P., Kenyon S. J., Hartmann L., Strom S. E., Edwards S., et al. (1991) *Astrophys. J.*, 382, 617-635.
- Hartmann L., Cassen P., and Kenyon S. J. (1997) *Astrophys. J.*, 475, 770-785.
- Henriksen R., Andre P., and Bontemps S. (1997) *Astron. Astrophys.*, 323, 549-565.
- Hillenbrand L. A. and White R. J. (2004) *Astrophys. J.*, 604, 741-757 (HW).
- Johns-Krull C. M., Valenti J. A., and Koresko C. (1999) *Astrophys. J.*, 516, 900-915 (J99).
- Johns-Krull C. M., Valenti J. A., and Saar S. H. (2004) *Astrophys. J.*, 617, 1204-1215.
- Jones H., Pavlenko Y., Viti S., and Tennyson, J. (2002) *Mon. Not. R. Astr. Soc.*, 330, 675-684.
- Leggett S. K., Allard F., Berriman G. Dahn C. C., and Hauschildt P. H. (1996) *Astrophys. J. Suppl.*, 104, 117-143.
- Ludwig H., Allard F., and Hauschildt P. H. (2002) *Astron. Astrophys.*, 395, 99-115.
- Ludwig H., Allard F. and Hauschildt P. H. (2006) *Astron. Astrophys.*, submitted.
- Luhman K. and Potter D. (2006) *Astrophys. J.*, in press.
- Luhman K., Stauffer J. and Mamajek E. (2005) *Astrophys. J.*, 628, L69-L72.
- Luhman K. L., Stauffer J. R., Muench A. A., Rieke G. H., Lada E. A., et al. (2003) *Astrophys. J.*, 593, 1093-1115.
- Magni G. and Mazzitelli I. (1979) *Astron. Astrophys.*, 72, 134-147.
- Mamajek E. E., Lawson W. A., and Feigelson E. D. (2000) *Astrophys. J.*, 544, 356-374 (M00).
- Mohanty S., Basri G., Jayawardhana R., Allard F., Hauschildt P., and Ardila D. (2004a) *Astrophys. J.*, 609, 854-884.
- Mohanty S., Jayawardhana R., and Basri G. (2004b) *Astrophys. J.*, 609, 885-905.
- Mohanty S., Jayawardhana R., and Basri G. (2005) *Astrophys. J.*, 626, 498-522.
- Mullan D.J. and MacDonald J. (2001) *Astrophys. J.*, 559, 353-371.
- Muzerolle J., Hillenbrand L., Calvet N., Briceno C., and Hartmann L. (2003) *Astrophys. J.*, 582, 266-281.
- Nordlund A. and Stein R.F. (1999) In *Theory and Tests of Convection in Stellar Structure* (A. Gimenez, E. F. Guinan, and B. Montesinos), pp. 91-102. ASP Conference Series, v. 173, San Francisco.
- Palla F. and Stahler S. W. (1999) *Astrophys. J.*, 525, 772-783 (PS99)
- Palla F. and Stahler S. W. (2001) *Astrophys. J.*, 553, 299-306.
- Pavlenko Y. V., Rebolo R., Martin E. L., and Garcia Lopez R. J. (1995) *Astron. Astrophys.*, 303, 807-818.
- Perrin G., Coude Du Foresto V., Ridgway S. T., Mariotti J.-M., et al. 1998, *Astron. Astrophys.*, 331, 619-626.
- Pols O. R., Tout C. A., Eggleton P. P., and Han Z. (1995) *Mon. Not. R. Astr. Soc.*, 274, 964-974.
- Pont F., Melo C. H. F., Bouchy F., Udry S., Queloz D., et al. (2005) *Astron. Astrophys.*, 433, L21-L24.
- Popper D. (1987) *Astrophys. J.*, 313, L81-L83 (P87).
- Prato L., Simon M., Mazeh T., McLean I. S., Norman, D., and Zucker, S. (2002) *Astrophys. J.*, 569, 863-871 (P02).
- Rucinski S.M. (1999) in *IAU Coll.170, Precise Stellar Radial Velocities* (J.B. Hearnshaw and C.D.Scarfe, eds.), pp. 82-90. ASP Conference Series, v. 185, San Francisco.
- Reiners A., Basri G., and Mohanty S. (2005) *Astrophys. J.*, 634, 1346-1352.
- Saumon D., Chabrier G., and Van Horn H. M. (1995) *Astrophys. J. Suppl.*, 99, 713-741.
- Schaefer G. (2004) Ph.D. dissertation, State University of New York at Stony Brook.
- Siess L., Dufour E., and Forestini M. (2000) *Astron. Astrophys.*, 358, 593-599 (SDF00).
- Simon K.P., Sturm E., and Fiedler, A. (1994) *Astron. Astrophys.*, 292, 507-518.
- Simon M. (2006) In *ESO Workshop on The Power of Optical/IR Interferometry* (F. Paresce and A. Richichi, eds.), in press.
- Simon M., Dutrey A., and Guilloteau S. (2000) *Astrophys. J.*, 545, 1034-1043 (Si00).
- Simon M. and Prato L. (2004) *Astrophys. J.*, 613, L69-L71.
- Slesnick C., Hillenbrand L., and Carpenter J. M. (2004) *Astrophys. J.*, 610, 1045-1063.
- Song I., Bessell M., and Zuckerman B. (2002) *Astrophys. J.*, 581, L43-L46.
- Stahler S. (1988) *Astrophys. J.*, 332, 804-825.
- Stassun K. G., Mathieu R. D., and Valenti, J. (2006) *Nature*, in press (S06).
- Stassun K. G., Mathieu R. D., Vaz L. P. R., Stroud N., and Vrba F. J. (2004) *Astrophys. J. Suppl.*, 151, 357-385 (S04).
- Steffen A. T., Mathieu R. D., Lattanzi M. G., Latham D. W., Mazeh T., et al. (2001) *Astron. J.*, 122, 997-1006 (St01).
- Strom K. M., Strom S. E., Edwards S., Cabrit S., and Skrutskie M. F. (1989) *Astron. J.*, 97, 1451-1470.
- Swenson F. J., Faulkner, J., Rogers, F. J., and Iglesias, C. A. (1994) *Astrophys. J.*, 425, 286-302 (S94).
- Torres G., Sandberg C. H., Marshall L. A., Sheets H.A., and Mader, J.A. (2006) *Astrophys. J.*, submitted.
- Ventura P., Zeppieri A., Mazzitelli I., and D'Antona F. (1998) *Astron. Astrophys.*, 331, 1011-1021.
- White R. J., Ghez A. M., Reid I. N., and Schultz G. (1999) *Astrophys. J.*, 520, 811-821.
- White R. and Hillenbrand L. (2005) *Astrophys. J.*, 621, L65-L68.
- Yang H., Johns-Krull C.M., and Valenti, J.A. (2005) *Astrophys. J.*, 635, 466-475.
- Zucker S. and Mazeh T. (1994) *Astrophys. J.*, 420, 806-810.
- Zuckerman B. and Song I. (2004) *Ann. Rev. Astron. Astrophys.*, 42, 685-721.